Elucidating the Nature of the Excited State of a Heteroleptic Copper Photosensitizer Using Time-Resolved X-ray Absorption Spectroscopy

Dooshaye Moonshiram*[a], Pablo Garrido-Barros[a,b], Carolina Gimbert-Suriñach[a], Antonio Picón[c,d], Cunming Liu[e], Xiaoyi Zhang[e], Michael Karnahl*[f], and Antoni Llobet*[a,g].

Abstract: We report the light-induced electronic and geometric changes taking place within a heteroleptic Cu(I) photosensitizer, namely [(xant)Cu(Me_2phenPh_2)]PF_6 (xant = xantphos, Me_2phenPh_2 = bathocuproine), by time-resolved X-ray absorption spectroscopy in the ps-μs time-regime. Time-resolved X-ray absorption near edge structure (XANES) and extended X-ray absorption fine structure (EXAFS) analysis enabled the elucidation of the electronic and structural configuration of the copper centre in the excited state as well as its decay dynamics in different solvent conditions with and without triethylamine acting as a sacrificial electron donor. A three-fold decrease in the decay lifetime of the excited state is observed in the presence of triethylamine showing the feasibility of the reductive quenching pathway in the latter case. A prominent pre-edge feature is observed in the XANES spectrum of the excited state upon metal to charge ligand transfer transition indicating an increased hybridization of the 3d states with the ligand p orbitals in the tetrahedron around the Cu centre. EXAFS and Density Functional Theory (DFT) illustrate the local geometrical configuration of the excited state showing a significant shortening of the Cu-N and an elongation of the Cu-P bonds together with a decrease in the torsional angle between the Xantphos and bathocruproine ligand. This study provides mechanistic time-resolved understanding for the development of improved heteroleptic Cu(I) photosensitizers, which can be used for the light-driven production of hydrogen from water.

Introduction

The production of solar fuels by using the energy of the sun is one of the most urgent scientific challenges in view of the rapid depletion of fossil fuels, the resulting environmental pollution and climate change.[1] Although today's state of the art technology has made considerable progress in producing electricity using sunlight and wind, these intermittent sources will only find limited applications without efficient energy storage.[1c, 2] One capable way to store solar energy is to convert it into chemical energy through fuel forming reactions inspired by natural photosynthesis, such as the light induced splitting of water into hydrogen and oxygen ($2\ H_2O + 4h\upsilon = O_2 + 2\ H_2$).[3] Indeed, the prospect of using molecular hydrogen has motivated the development and application of light harvesting units for solar H_2 generation in both metal-complex chromophores and molecular photocatalysts.[4]

While most of the molecular photosensitizers are based on noble-metals, such as Ru(II), Ir(III), Pt(II), Au(III) and Re(I), some work on cheaper and more abundant 3d transition metals like Cu(I), Cr(III) and Zn(II) porphyrin complexes have also been reported.[4a, 4b, 5] In this respect, novel heteroleptic Cu(I) photosensitizers of the general type $[(P\hat{}P)Cu(N\hat{}N)]^+$ composed of a diimine N^N and a bulky diphosphine P^P ligand have attracted particular interest as they allow for considerable photocatalytic activities in conjunction with an Fe-based water reduction catalyst.[6]

The design of these heteroleptic Cu(I) complexes is an ongoing area of research that has experienced a significant development during the last years with respect to their well-known homoleptic counterparts of the type $[Cu(N\hat{}N)_2]^+$ (Scheme 1A and 1B).[5a, 5d, 6a, 7] The properties of the homoleptic bis-diimine photosensitizers are already extensively studied since decades[8] due to their tuneable photophysical and electrochemical properties. These photosensitizers are found to undergo a structural reorganization upon photoexcitation from a pseudo tetrahedral geometry to a flattened state (flattening distortion)[9] enabling the coordination of a solvent molecule to the Cu centre. As a result, a low-energy excited state is formed, known as an "exciplex", which exhibits a fast emission decay to the ground state with shortened excited state lifetimes in the order of ps-ns.[5a, 9a, 9b]. While significant advances have been made in the fine-tuning of the diimine ligands[8a, 8c, 8g, 10] and the improvement of the resulting bis-diimine complexes these homoleptic Cu(I) compounds have only found restricted use in the photocatalytic reduction of protons from water.[7c, 11] In contrast, a large number of the heteroleptic ones exhibit increased excited state lifetimes, which even exceed some of the commonly applied Ru(II) photosensitizers.[5a, 6b, 7a, 12] In addition, the properties of these heteroleptic complexes can be tuned in a broader range due to the presence of two distinct ligands compared with their homoleptic counterparts. For instance, it was found that both the photocatalytic activity and emission lifetime strongly improved upon addition of bulkier substituents at the 2,9-position of the phenanthroline ligand (Scheme 1).[6b, 7a, 12a, 13] Replacement of the two methyl groups by *sec*-butyl considerably increased the turnover number of hydrogen production from 862 to 1330 as well as the emission lifetime of the triplet excited state from 6.4 µs to 54.1 µs (in degassed THF solution).[6b, 12a]

However, in spite of emerging design principles and active synthetic efforts in developing advanced heteroleptic copper-based photosensitizers, there is an urgent need to correlate their performance and stability to the underlying geometric structures for rational developments in the future. Although the photophysical and structural properties of these heteroleptic copper photosensitizers have been studied by different techniques such as optical transient absorption[6c, 7c], UV-vis[6b, 6e, 7b, 7d, 7f, 7h-j, 7l, 14], resonance Raman[6e], electrochemistry[6e, 7e, 7h, 7j, 7l], single crystal X-ray diffraction[7f, 7i, 7l, 14-15], mass spectrometry[15], NMR[6f, 7f, 7g, 13, 15] and EPR spectroscopy[6f], the geometrical reorganization of the triplet excited state has not yet been experimentally demonstrated. Elucidation of the nature of the excited state through direct experimental proof is however crucial. Moreover, although disproportionation of heteroleptic $[Cu(N\hat{}N)(P\hat{}P)]^+$ complexes to form homoleptic species in solution has been proposed[6e, 6f, 7g], structural analysis of the excited state which could lead to the degradation pathway of this class of Cu(I) photosensitizers has not yet been performed.

In this regard, synchrotron-based X-ray absorption spectroscopy (XAS) has proven to be a powerful tool for tracking electronic and geometrical changes within molecules.[16] XAS has further been extended to the ultrafast time domain for time-resolved laser (pump), X-ray (probe) experiments through the usage of lasers with high power and high repetition rate. In this technique, a short laser pulse excites molecules within a liquid and the ~100 ps X-ray pulses capture the transient states of the molecule as it evolves.[17] Nowadays, these high-repetition-rate laser systems can also produce short fs-ps pulses, which when combined with the high-repetition rate of the X-rays allows full utilization of the X-ray flux.[17a]. This capability has been implemented at various beamlines around the world such as the SLS[18] (Switzerland), BESSY[19] (Germany), Petra III[20] (Germany), Elettra[21] (Italy), ALS[22] (U.S.A), APS[17b, 23] (U.S.A) and the Photon factory (Japan)[24], enabling the use of time-resolved hard X-ray absorption spectroscopic (tr-XAS) tools with ps-µs temporal resolution in both the soft and hard X-ray range. Tr-XAS has been used to capture snapshots of transient states in many photocatalytically relevant complexes, and has considerably enhanced the fundamental understanding of photochemistry, solar energy conversion, interfacial electron transfer processes and biological enzymatic systems[22b, 22c, 24-25]

The present study elucidates the light-induced electronic and structural dynamics leading to the formation of the excited state (as presented in Scheme 1C) derived from the heteroleptic copper photosensitizer $[(xant)Cu(Me_2phenPh_2)]PF_6$ (with xant =

[a] Dr. D. Moonshiram*, Mr. P. Garrido-Barros, Dr. C. Gimbert Suriñach, Prof. Dr. A. Llobet*
Institute of Chemical Research of Catalonia (ICIQ), Avinguda Països Catalans 16, 43007 Tarragona, Spain
E-mails: dmoonshi@gmail.com, allobet@iciq.cat
[b] Mr. P. Garrido-Barros
Departament de Química Física i Inorganica, Universitat Rovira i Virgili, Campus Sescelades, C/Marcellí Domingo, s/n, 43007, Tarragona, Spain
[c] Dr. A. Picón
Grupo de Investigacion en Aplicaciones del Laser y Fotonica, Departamento de Fisica, Aplicada, Universidad de Salamanca, 37008, Salamanca, Spain
[d] Dr. A. Picón
ICFO, Institut de Ciences Fotoniques, The Barcelona Institute of Science and Technology, 08860, Castelldefells, Barcelonia, Spain
[e] Dr. C.Liu, Dr. X.Zhang
X-ray Science Division, Argonne National Laboratory, 9700 S. Cass Avenue, Lemont, IL, 60439, U.S.A
[f] Prof. Dr. M. Karnahl*
University of Stuttgart, Institute of Organic Chemistry, Pfaffenwaldring 55, 70569, Stuttgart, Germany
Email: michael.karnahl@uni-stuttgart.de
[g] Prof. Dr. A. Llobet*
Departament de Química, Universitat Autonoma de Barcelona, 08193 Cerdanyola del Valles, Barcelona, Spain

Supporting information for this article is given via a link at the end of the document. This includes pre-edge XAS calculations, EXAFS simulations, EXAFS analysis, and DFT optimized coordinates.

xantphos and $Me_2phenPh_2$ = bathocuproine). XANES, EXAFS and time-correlated single photon counting experiments in combination with DFT calculations are used to reveal critical electronic and structural information about the Cu-MLCT state and its dynamics in the presence and absence of an electron donor. To the best of our knowledge, time-resolved X-ray absorption spectroscopy studies of heteroleptic copper complexes of the type $[(P\text{^}P)Cu(N\text{^}N)]^+$ have not been reported prior to this work. Therefore, the findings of this study constitute an important step towards elucidating the structural configuration of the excited state with the aim of improving the design of heteroleptic copper photosensitizers resulting in higher chemical stabilities and photocatalytic activities.

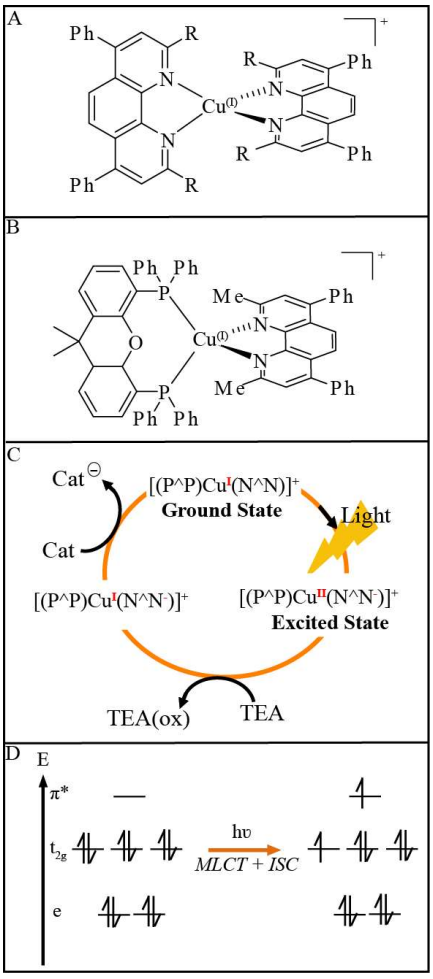

Scheme 1 A. General structure of common homoleptic Cu(I) bis-diimine complexes **B.** Heteroleptic copper photosensitizer investigated in this study, $[(xant)Cu(Me_2phenPh_2)]PF_6$ (with xant = xantphos, $Me_2phenPh_2$ = bathocuproine) **C.** Proposed reaction mechanism for the photocatalytic production of hydrogen applying the copper photosensitizer $[(xant)Cu(Me_2phenPh_2)]PF_6$ **D.** Simplified molecular orbital scheme of Cu(I) photosensitizers upon light excitation adapted from [26].

Results and Discussion

Time-resolved XANES: copper oxidation and metal-to-ligand charge transfer transitions. Formation of the excited state of $[(xant)Cu(Me_2phenPh_2)]PF_6$ after illumination was probed in the ps-µs time range by time-resolved laser/X-ray pump/probe spectroscopy of the copper complex in a THF/H_2O solvent mixture (volume ratio of 9:1) as well as in a mixture of $THF/TEA/H_2O$ (volume ratio of 4:3:1). The latter mixture including triethylamine as electron donor was chosen as it had previously been proven to give the best catalytic results in combination with $[Fe_3(CO)_{12}]$ as water reduction catalyst.[6b, 6d, 12a] The Cu(I) complex in both solution mixtures was optically pumped at 400 nm with a 10 kHz repetition rate laser and probed with X-ray pulses at varying time delays ranging from 100 ps to 30 µs.

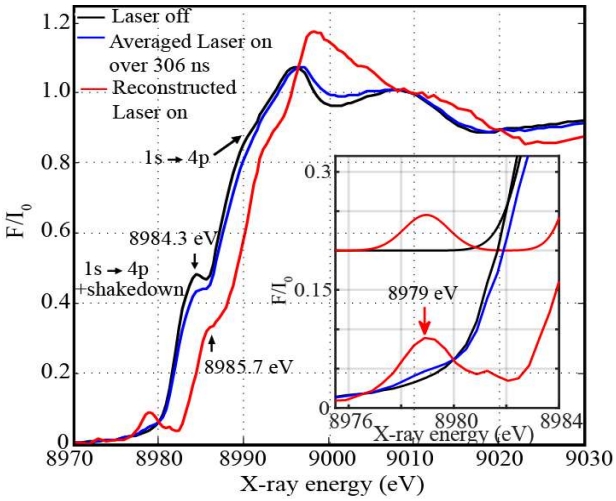

Figure 1. Experimental transient X-ray absorption spectrum of the heteroleptic Cu(I) photosensitizer before laser excitation (black) and measured at an averaged time delay of 100 ps-306 ns after laser excitation (blue). The reconstructed spectrum of the excited state was calculated considering an excitation percentage of 17.5 % (red, see main text). **Inset**. **Top**. Calculated Time-dependent Density Functional Theory (TD-DFT) pre-edge simulations for the ground and excited state from optimized calculations (Table 1). **Bottom**. Zoom of the experimental pre-edge features

The XANES spectra were collected before (laser off) and after (laser on) laser excitation. The laser-on XAS spectrum for an averaged time delay of 100 ps-306 ns between the laser pump excitation and the X-ray probing is shown in Figure 1. Upon light excitation, metal-to-ligand-charge-transfer (MLCT) causes an electronic transition from the 3d orbital of Cu(I) to the π*-orbital of the phenanthroline ligand followed by intersystem crossing to a triplet excited state (Scheme 1 C,D).[6c, 9a, 9b] The MLCT transition causes a formal oxidation of the copper centre from Cu(I) to Cu(II) and a reduction of the diimine ligand forming an intermediate $[(P\text{^}P)Cu^{II}(N\text{^}N^-)]PF_6$ species (see Scheme 1 C,D). The formation of the excited state was illustrated by the copper XANES spectra, which are generally characterized by two peaks along the rising maximum edge, namely the 1s → 4p "main" peak along with a

secondary peak due to a 1s→ 4p transition with shakedown contributions.[27] These shakedown effects involve ligand to metal charge transfer states during the relaxation of the Cu local electrons in the excited state.[27] The comparison of the laser on, and the laser off XANES spectra shows a clear positive energy shift of around 0.53 eV at around half height and 0.5 normalized absorption, reflecting the higher ionization energy required for ejecting a core 1s electron from a more positively charged ion. The excited state fraction of $[(P\text{^}P)Cu^{II}(N\text{^}N^{-})]^{+}$ was determined by comparing its XANES spectrum to those of previously reported $[Cu(dmp)_2]^{+}$ complexes[8e, 9a, 28] (where dmp = 2,9-dimethyl-1,10,phenanthroline) and typical reference Cu(I) and Cu(II) complexes with similar coordination environment. A relative chemical shift in energy of around 3 eV is typically obtained between those Cu(I) and Cu(II) reference complexes[29] such that a proportion of the excited state of around 17.5 % was estimated in the laser on spectrum of $[(P\text{^}P)Cu^{II}(N\text{^}N^{-})]^{+}$, and further used to plot the actual or reconstructed spectrum of the excited state (Figure 1, red line). The reconstructed excited state exhibits a pre-edge transition at 8979.0 eV and the 1s→ (4p+shakedown) rising-edge transition at 8985.7 eV which are in good agreement with previously reported four-coordinate Cu(II) ions[29-30], thus confirming the correct proportion of excited state fraction used in the estimation of the laser on spectrum.

Interestingly, the XANES spectrum not only shows a clear change in the formal oxidation state of the copper centre but also striking changes in the electronic configuration and local site geometry as demonstrated by the prominent pre-edge feature (Figure 1 inset). Presence of pre-edge features correspond to 1s to 3 d quadrupole transitions which are formally dipole forbidden but gain intensity due to 4 p mixing into the Cu 3d-shell.[31] The tetrahedral Cu(I) ground state has a d^{10} orbital configuration with filled e_g and t_{2g} levels. Upon light excitation, metal to ligand charge transfer triggers an electron to be promoted to the low lying π*-orbital of the phenanthroline ligand, thus causing the occupation of the Cu d level to change as illustrated in Scheme 1D. The d level atomic rearrangements in the excited state are additionally accompanied with structure relaxation, and increased hybridization of the valence 3 d states with N/P ligand p orbitals explaining the presence of the prominent pre-edge feature at 8979 eV.[31c, 31d] Pre-edge calculations from DFT optimized coordinates were carried out for both the Cu(I) ground and excited state and reproduced the experimental data well (Figure 1 inset, Figure S1). Since the pre-edge peak intensity of the Cu(I) excited state's is too large to arise only from electric quadrupole transitions as illustrated in Figure S1, this feature gains further intensity through 4p→ 3d mixing, and the substantially more intense dipole allowed 1s→ 4 p character contribution to this transition (Figure 1, S1). The pre-edge calculation shown here further ascertains that geometry optimization and ab-initio XAS simulations used for the Cu photosensitizer can be reliably used for analysis of the Cu(I) excited state.

Time-resolved EXAFS and DFT calculations: Structural configuration around the copper centre. As previously noted, unlike in homoleptic Cu(I) complexes, the bulky diphosphine ligand of the heteroleptic copper photosensitizer inhibits flattening distortion of the $3d^9$ configuration of the excited state. Thus, due to steric hindrance, the formally Cu(II) MLCT state maintains its geometrical configuration instead of the usual flattened geometry observed for analogous homoleptic complexes. The copper centre is consequently less susceptible to nucleophilic attack by solvent molecules and exciplex formation, which have been known to lead to shorter excited state lifetimes in their homoleptic counterparts.[5a, 8e, 9a, 28b]

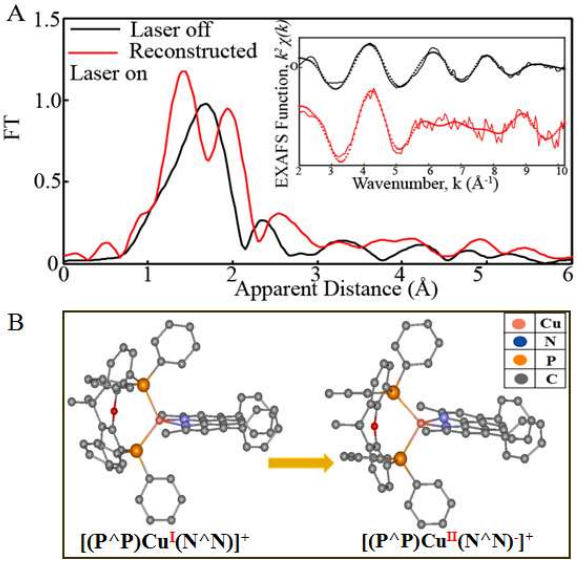

Figure 2 A. Fourier transforms of k^2-weighted Cu EXAFS of the laser off (black) and reconstructed excited state, considering a 17.5 % excited state fraction (red). **Inset**: Back Fourier transforms, experimental results (solid lines), and fitting (dotted marked lines) k^2 χ(k) Fourier transforms were calculated for k values of 2- 10.2 $Å^{-1}$. **C.** Calculated structures of the Cu(I) complex in the ground and the excited state. Hydrogen atoms are omitted for clarity.

The EXAFS spectra of the heteroleptic Cu(I) photosensitizer and its derived excited state are shown in Figure 2 A. Analysis of the Cu(I) complex reveals a prominent peak in the first coordination sphere corresponding to summed contribution of the Cu-N and Cu-P bond distances. On the other hand, two prominent peaks are observed for the excited state derivative corresponding to the distinct contribution of the shortened Cu-N and elongated Cu-P bonds. EXAFS fits for the first coordination sphere and the entire spectrum are shown in tables 1,S1. Analysis of the first peak in the excited state clearly resolves the Cu-N distances at 2.09 Å. Furthermore, the inclusion of two Cu-P distances at 2.27 Å improves the quality of the fit as shown by the decreased R-factors and reduced chi-squared values (Table 1, S1, fit 2). Similarly, fitting of the

excited state illustrates an improvement of the fit quality after addition of two shortened Cu-N distances at 1.91 Å and elongated Cu-P distances at 2.36 Å (Table 1, S1, fit 6). The fitted Cu-N and Cu-P bond distances are in agreement with the reported single crystal X-ray diffraction (XRD) structure[32], and relative trends between the relaxed structures from Density Functional Theory (DFT) geometry optimization (Table 1, S2).

Table 1. Comparison of structural parameters from EXAFS

Species, Fit No. in Table S1	EXAFS Shell: N x distance in Å/ Error bars (100th Å)	XRD (Å)[32] [a]	DFT Optimized Coordinates (Å) (Table S2,SI)
Cu(I) Ground state (Fit 3)	Cu-N, 2: 2.04(1) Cu-P,2 : 2.27(2) Cu-C, 4: 2.93(3) Cu-C, 8: 3.14(3)	$Cu\text{-}N_1$: 2.06 $Cu\text{-}N_2$: 2.10 Cu-P1: 2.24 Cu-P2: 2.30 N-Cu-N: 80.6˚ P-Cu-P: 119.9˚ Torsional Angle = 85.0˚	$Cu\text{-}N_1$: 2.10 $Cu\text{-}N_2$: 2.12 $Cu\text{-}P_1$: 2.23 $Cu\text{-}P_2$: 2.29 N-Cu-N: 79.9˚ P-Cu-P: 122.3˚ Torsional angle = 84.6 ˚
Excited State (Fit 6)	Cu-N, 2: 1.91(2) Cu-P, 2: 2.36(2) Cu-C, 4: 3.05(3) Cu-C, 8: 3.14(3)		$Cu\text{-}N_1$: 1.99 $Cu\text{-}N_2$: 2.01 $Cu\text{-}P_1$: 2.38 $Cu\text{-}P_2$: 2.38 N-Cu-N: 83.4˚ N-Cu-P: 102.0˚ Torsional angle = 71.6˚

[a] XRD data of $[(xant)Cu(Me_2phenPh_2)]PF_6$ was taken from reference [32] for comparison. CCDC1561239 contains the crystallographic data of this complex, which is provided free of charge by the Cambridge Crystallographic Data Centre.

DFT calculations of the excited state further show a pronounced distorted geometry around the copper centre compared to the ground state, which is in agreement with the EXAFS results discussed above. For instance, the N-Cu-N bite angle increases from 79.9˚ to 83.4˚, whereas the P-Cu-P angle decreases considerably by 20.3˚ from 122.3˚ to 102.0˚. The high degree of distortion is also evident from the angle between the two planes which are formed by the xantphos and the bathocuproine ligand that decreases from 84.6˚ to 71.6˚ as depicted in Figure 2B. This decrease of the so-called ligand plane intersection angle is in agreement with previous findings.[6c, 32] Furthermore, the stepwise decomposition of the original heteroleptic photosensitizer, and the formation of its homoleptic $[Cu(N^N)_2]^+$ counterpart in solution has been revealed through by a range of spectroscopic techniques such as UV-Vis spectroscopy[6e, 7k], hydrogen evolution studies under various solvent conditions[7k], electrochemistry[6f, 7h], resonance rRaman spectroscopy[6e], Electron Paramagnetic Resonance[6f], and Nuclear Magnetic Resonance[[6f, 7g13] studies. While the XANES and EXAFS analysis of the decomposition product is outside the scope of this manuscript, the elongation of the Cu-P bond distances and P-Cu-P bite angle could provide a first hint towards the ligands' dissociations in the heteroleptic Cu(I) photosensitizer and its degradation pathway.

Excited state lifetime. The excited state is formed in less than ~100 ps, which corresponds to the pulse duration of the X-rays in the tr-XAS experiment. The decay of the excited state's transient signal was monitored at varying time points between 100 ps to around 5.4 µs. Features in the tr-XAS spectra obtained by subtracting the laser-on and laser-off (dark) spectra provide further information about the excited state. Figures 3 A and B show the tr-XAS spectra at varying time delays of 100 ps, 612 ns and 1.683 µs between the laser and X-ray pulses. Two prominent features are obtained in the transient signal at 8983.2 and 8988.9 eV related to the changes in the 1s → (4p + shakedown) transition along with the 1s → 4p main transition. These transitions point towards the ground state bleaching of the Cu(I) photosensitizer. Moreover, two broad peaks at 8999.1 eV and 9016.6 eV relate to the formation of the formally oxidized Cu(II) species. These energy transitions show that the K-edge of the Cu centre shifts to higher energy, indicating the oxidation of Cu(I) and confirming the electron transfer from the 3d orbital of Cu(I) to the π*-orbital of the bathocuproine ligand. Lastly a pre-edge peak is observed at 8979 eV related to the increased hybridization of the core electrons into the valence 3d states hybridized with N/P ligand orbitals as elaborated above.

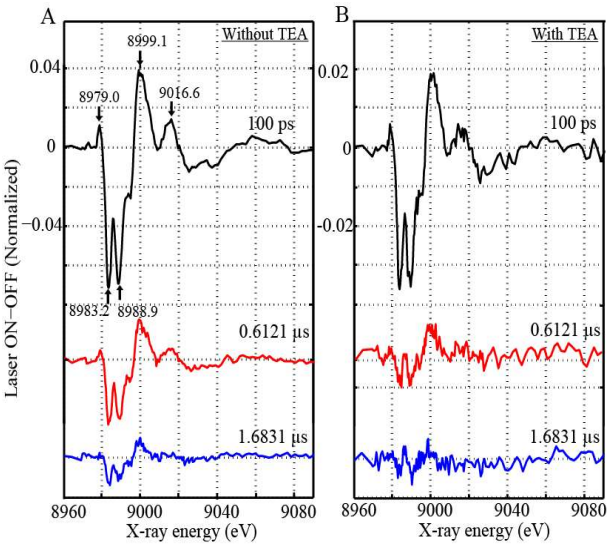

Figure 3. Experimental difference spectrum corresponding to the excited state due to MLCT at a series of time delays between laser and X-ray pulses for a mixture consisting of **A**. 1 mM Cu(I) photosensitizer in a solvent mixture of THF/H_2O with a volume ratio of 9:1 . **B**. 1 mM Cu(I) photosensitizer in a solvent mixture of THF/TEA/H_2O with a volume ratio of 4:3:1.

The kinetics and decay of the excited state in the absence and presence of triethylamine (TEA), acting as electron donor, was additionally monitored. As illustrated in Figure 4 A, the photon energy was fixed to around 9000 eV corresponding to the formation of the excited state and the time-delays between the laser and X-ray pulses varied. The formation of the Cu(II) MLCT

state appears promptly in less than the ~100 ps pulse duration of the X-rays and decays within 1095 ± 87 ns in a solution mixture of THF/H_2O (Figure 3A, 4A). However, in the presence of TEA, the excited state decays much faster by a factor of around 3, within 375 ± 129 ns, indicating the quicker generation of the Cu(I) reduced state, [(P^P)Cu^I(N^N)] (Scheme 1, Figures 3B,4A). The shorter decay time of the excited state in the presence of TEA confirms that reductive quenching is fast and may have a significant contribution in photochemical hydrogen evolution reactions.[6b] The emission decays of the excited state in the absence and presence of the sacrificial reductant were also studied by time-correlated single photon counting (TCSPC) measurements (Figure 4 B). Decay times of 1170 ± 5 ns (without TEA) and 382 ± 1 ns (with TEA) were obtained, which are in agreement with previous observations and the proposed reaction mechanism.[6b]

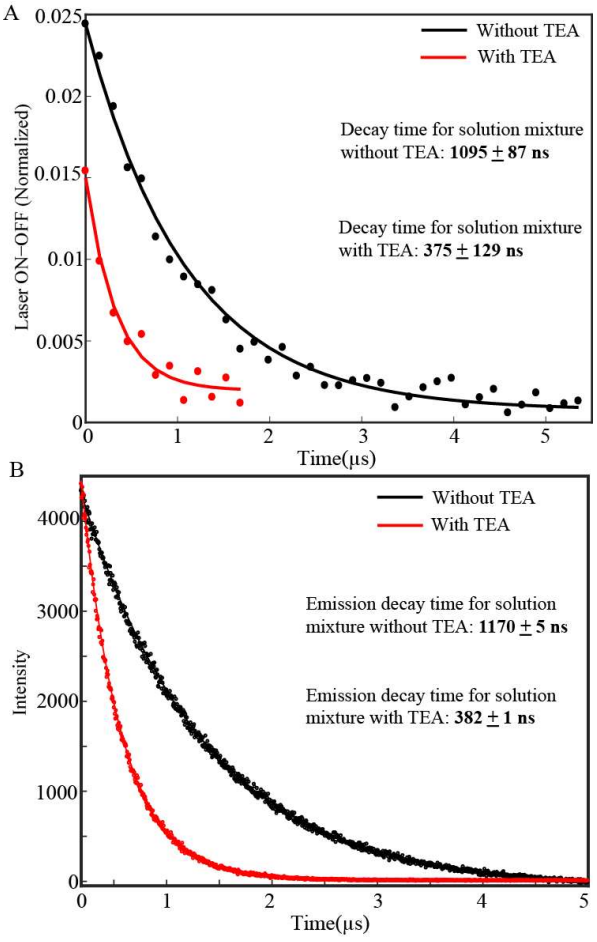

Figure 4 A. Pump-probe delay scan recorded at peak energy of the excited state's transient signal, corresponding to the excited state's formation in the absence (black) and in the presence (red) of the sacrificial electron donor triethylamine. **B.** Emission decay of the excited state (monitored at 586 nm) of 0.1 mM Cu(I) photosensitizer in a solvent mixture of THF/H_2O with a volume ratio of 9:1 (black) and a solvent mixture of THF/TEA/H_2O with a volume ratio of 4:3:1 (red).

Summary and Conclusions

In summary, we trapped and elucidated the structure of the excited state of one of the most efficient heteroleptic diimine-diphosphine Cu(I) complexes [(xant)Cu(Me_2phenPh_2)]$^+$ used for the photocatalytic production of hydrogen by time-resolved X-ray absorption spectroscopy (tr-XAS). XANES in combination with EXAFS analysis revealed the local electronic and structural configuration of the copper centre in the excited state. Importantly, the excited state reveals a Cu-P bond length elongation of 0.13 Å and a Cu-N bond length reduction of 0.09 Å. This change is in agreement with the DFT calculations, which show a much more pronounced distorted tetrahedral geometry in the excited state and decreased P-Cu-P bite angle. For instance, the angle between the two planes formed by the xantphos and bathocuproine ligand in the ground state is around 84.6˚, whereas in the excited state this angle distorts only to around 71.6˚ as compared to around 59˚ in homoleptic photosensitizers of the type [Cu^I(dmp)$_2$]$^+$ (with dmp = dimethylphenanthroline).[28b] This is in agreement with the longer lifetime of the excited state in this class of heteroleptic Cu(I) photosensitizers due to their lower propensity to exciplex formation. However, the reduced stability of the heteroleptic diimine-diphosphine Cu(I) photosensitizers with regard to the homoleptic bis-diimine counterparts could be due to the elongation of the Cu-P bond in the excited state that leads towards a stepwise decomposition during photocatalysis.[6c, 6e, 6f, 7g]

The decay kinetics of the excited state was also studied with tr-XAS and TCSPC techniques giving lifetimes of the order of microseconds. This is in contrast to the broad range of analogous homoleptic bis-diimine Cu(I) complexes, that have vastly been studied through both ultrafast optical and tr-XAS spectroscopy[8e, 8g, 9a, 28] revealing emission lifetimes only in the order of nanoseconds.

Importantly, this study outlines the necessity to further enhance the stability of heteroleptic Cu(I) photosensitizers by the right choice of the diphosphine ligand. Furthermore, the application of bulkier and more rigid ligands supports to avoid undesired flattening distortion of the excited state as well as exciplex quenching. This work also provides future promise of elucidating key processes in the order of femtosecond-sub picoseconds times scales such as metal-to-ligand-charge-transfer and intersystem crossing. Such processes which occur before the formation of the excited state can, for instance, be studied at free electron laser facilities where femtosecond time resolution has become possible. These studies can identify critical factors influencing the structural reorganization of the copper centre in the excited state and better control the energetics of the MLCT charge transfer and dynamics of the intersystem crossing rates upon light excitation.

Experimental Section

Sample Preparation. The heteroleptic copper photosensitizer [(xant)Cu(Me_2phenPh_2)]PF_6 was synthesized as previously described and matched all reported characterization.[6b, 6d] Ultrapure water (type 1, with a resistivity of 18.2 MΩ.cm at 25°C, total organic carbon content of 4 µg/L) sourced from a Q-POD unit of Milli-Q integral water purification system (Millipore) was used. The respective solvent mixtures were prepared applying anhydrous > 99 % pure tetrahydrofuran (Catalog No. 401757, Sigma Aldrich) and > 99 % pure triethylamine (Catalog No. T0886, Sigma Aldrich).

Time-resolved XAS measurements. Time-resolved X-ray absorption spectra were collected at 11 ID-D[17b] beamline at the Advanced Photon Source using undulator radiation at electron energy 9.0 keV. The experiments were carried out using the 24 bunch timing mode of APS (in top up mode with a constant 102 mA ring current) which consists of a train of X-rays separated by 153 ns. This mode easily allows for gateable detectors that selects X-ray pulses.

The sample was pumped at 400 nm wavelength using a regenerative amplified laser with 10 kHz repetition rate 5ps-FWHM pulse length and laser power of 397 mW. The sample was circulated through a stainless steel nozzle into a free-flowing 550 µm cylindrical jet inside an airtight aluminium chamber, and continuously degassed with nitrogen. The X-ray and laser beam was spatially overlapped with an X-ray spot size of 100 µm(V) x 450 µm(H) and laser spot size of 170 µm(V) x 550 µm. With a liquid flow speed of 3 m/s, the pumped laser volume was calculated to move out of the FWHM region in around 30 µs. This temporal range ensured that the excited state volume was probed more at the centre and less at the edges where the excitation fraction would be less, due to movement of the sample. Beamline 11 ID-D has an automated data digitization system which allows for all X-ray pulses after laser excitation to be collected. Such a system, together with the larger X-ray beam spot size, was very useful for our experiments, as multiple X-ray pulses after laser excitation were averaged to monitor the dynamics for the formation and decay of the copper excited state species in the ns-µs time regime. In addition, by averaging multiple pulses, we obtained a better resolution of the main features in the pre-edge and edge regions of the transient signals.

The delay between the laser and X-ray pulses was adjusted by a programmable delay line (PDL-100A-20NS, Colby Instruments) and the X-ray fluorescence signals were collected with two APDs positioned at 90° on both sides of the liquid jet. Moreover, a combination of Z-1 filters and soller slits with conical geometry were used to reduce the background from elastically scattered X-rays. A Cu metal foil was placed between two ionization chambers downstream to the X-ray beam, and its transmission recorded with each scan for energy calibration.

Time-correlated single photon counting measurements. Time-correlated single photon counting experiments (TCSPC) measurements were carried out on an Edinburgh Instruments LifeSpec-II spectrometer, equipped with a PMT detector and a double subtractive monochromator. The Cu(I) L complex was pumped with 405 nm excitation with a 20 KHz picosecond pulsed diode laser source and its emission probed at 586 nm. The samples were measured in a 1 cm cuvette sealed with a septum cap and thoroughly degassed with N_2 gas.

EXAFS data analysis. Athena software [33]was used for data processing. The energy scale for each scan was normalized using copper metal standard. Data in energy space were pre-edge corrected, normalized, and background corrected. The processed data were next converted to the photoelectron wave vector (k) space and weighted by k^2. The electron wave number is defined as, $k = [2m(E-E_0)/\hbar^2]^{1/2}$ where E_0 *is* the energy origin or the threshold energy. K-space data were truncated near the zero crossings (k = 2-10.2 Å^{-1}) in Cu EXAFS before Fourier transformation. The k-space data were transferred into the Artemis Software for curve fitting. In order to fit the data, the Fourier peaks were isolated separately, grouped together, or the entire (unfiltered) spectrum was used. The individual Fourier peaks were isolated by applying a Hanning window to the first and last 15% of the chosen range, leaving the middle 70% untouched. Curve fitting was performed using *ab initio*-calculated phases and amplitudes from the FEFF8[34] program from the University of Washington *Ab initio*-calculated phases and amplitudes were used in the EXAFS equation[35]

$$\chi(k) = S_0^2 \sum_j \frac{N_j}{kR_j^2} f_{eff\_j}(\pi, k, R_j) e^{-2\sigma_j^2 k^2} e^{\frac{-2R_j}{\lambda_j(k)}} \sin(2kR_j + \phi_{ij}(k)) \quad (1)$$

where N_j is the number of atoms in the j^{th} shell; R_j the mean distance between the absorbing atom and the atoms in the j^{th} shell; $f_{effj}(\pi,k,R_j)$ is the *ab initio* amplitude function for shell j, and the Debye-Waller term $e^{-2\sigma_j^2 k^2}$ accounts for damping due to static and thermal disorder in absorber-backscatterer distances. The mean free path term reflects losses due to inelastic scattering, where $\lambda_j(k)$, is the electron mean free path. The oscillations in the EXAFS spectrum are reflected in the sinusoidal term , sin ($2kR_j + \phi_{ij}(k)$) where $\phi ij(k)$ is the *ab initio* phase function for shell j. This sinusoidal term shows the direct relation between the frequency of the EXAFS oscillations in k-space and the absorber-back scatterer distance. S_0^2 is an amplitude reduction factor. The EXAFS equation (Eq. 1) was used to fit the experimental Fourier isolated data (q-space) as well as unfiltered data (k-space) and Fourier transformed data (R-space) using N, S_0^2, E_0, R, and σ^2 as variable parameters**.** N refers to the number of coordination atoms surrounding Cu for each shell. The quality of fit was evaluated by R-factor and the reduced Chi^2 value. The deviation in E_0 ought to be less than or equal to 10 eV. R-factor less than 2% denotes that the fit is good enough[35] whereas R-factor between 2 and 5% denotes that the fit is correct within a consistently broad model. The reduced Chi^2 value is used to compare fits as more absorber-backscatter shells are included to fit the data. A smaller reduced Chi^2 value implies a better fit.

DFT Calculations. DFT optimization calculations were performed using the ORCA program package developed by Neese and co-workers[36] The DFT optimization reported in Table 1 was carried out using ORCA , B3LYP[37] as functional, the Zeroth Order Regular Approximation (ZORA) as previously reported[38] with def2-TZVP triple-zeta basis sets[39], and the atom-pairwise Grimme dispersion correction with the Becke-Johnson damping scheme[40] (D3BJ). Time-dependent DFT (TD-DFT) calculations for the XAS spectrum of the Cu pre-edge were performed using the same functional, basis sets and dispersion correction effects with dense integration grids, and the fully decontracted def2-TZVP/J[39] auxiliary basis set. The pre-edge absorption spectra from the TD-DFT calculations were shifted in energy by -7.5 eV relative to the experimental data and a broadening of 2.0 eV was applied to all calculated spectra. The donor orbitals for XAS calculations were chosen as Cu 1s and all virtual orbitals were selected as acceptor orbitals. Up to 150 roots were calculated. The calculated pre-edge spectrum contains contributions from electric quadrupole, electric dipole and magnetic dipole transitions. Further DFT optimizations with lesser precision as XRD reported coordinates were carried out using the BP86[41] and BLYP[42] functional, and are summarized in Table S2 and SI. Importantly, all optimizations trends between the ground and the excited state agree well with experimental data as illustrated in Table 1 and Table S2. A consistent decrease in the Cu-N and elongation in the Cu-P distances is observed upon formation of the Cu(I)* excited state. Furthermore, an increase in the N-Cu-N bite angle and considerable decrease in the P-Cu-P angle is obtained in all reported calculations (Table 1, S2). The degree of distortion between the ground and excited states is additionally evident from the decrease in the torsional angle between the xantphos and the bathocuproine ligand.

Acknowledgements

MINECO, FEDER and FCI are gratefully acknowledged for financial support (CTQ2016-80058-R, CTQ2015-73028-EXP, SEV 2013-0319, ENE2016-82025-REDT (FOTOFUEL), CTQ2016-81923-REDC (INTECAT). The authors thank the COST Action CM1202. P. G.-B. acknowledges "La Caixa" foundation for a PhD grant. A.P. acknowledges funding from the European Union's Horizon 2020 research and innovation program under the Marie Sklodowska-Curie Grant Agreement No. 702565. This research used resources of beamline 11 ID-D of the Advanced Photon Source (APS), a U.S. Department of Energy (DOE) Office of Science User Facility operated for the DOE Office of Science by Argonne National Laboratory under Contract No. DE-AC02- 06CH11357. The laser system at beamline 11-ID-D of APS was funded through New Facility and Mid-scale Instrumentation grants (PI: Lin X. Chen). X.Z. and C.L. acknowledge funding from DOE, Office of Science, Basic Energy Sciences, Chemical Sciences, Geosciences, and Biosciences Division under contract no. DE-AC02-06CH11357.

Keywords: Artificial Photosynthesis • Electron Transfer • Copper heteroleptic photosensitizers • Time-resolved X-ray absorption spectroscopy. Photocatalysis

References:

[1] a) A. Thapper, S. Styring, G. Saracco, W. Rutherford, B. Robert, A. Magnuson, W. Lubitz, A. Llobet, P. Kurz, A. Holzwarth, S. Fiechter, H. d. Grott, S. Campagna, A. Braun, H. Bercegol, V. Artero, *Green* **2010**, *3*, 43-57; b) N. Armaroli, V. Balzani, N. Serpone, in *Powering Planet Earth*, Wiley-VCH Verlag GmbH & Co. KGaA, **2013**, pp. 65-82; c) S. Berardi, S. Drouet, L. Francas, C. Gimbert-Suriñach, M. Guttentag, C. Richmond, T. Stoll, A. Llobet, *Chem. Soc. Rev.* **2014**, *43*, 7501-7519.

[2] a) Q. Schiermeir, J. Tollefson, T. Scully, A. Witze, O. Morton, *Nature* **2008**, *454*, 816-823; b) D. Moonshiram, Y. Pineda-Galvan, D. Erdman, M. Palenik, R. Zong, R. Thummel, Y. Pushkar, *J. Am. Chem. Soc.* **2016**, *138*, 15605-15616.

[3] a) N. S. Lewis, D. G. Nocera, *Proc. Natl. Acad. Sci.* **2006**, *103*, 15729-15735; b) N. Armaroli, V. Balzani, *Angew. Chem. Int. Ed.* **2007**, *46*, 52-66.

[4] a) P. D. Frischmann, K. Mahata, F. Wurthner, *Chem. Soc. Rev.* **2013**, *42*, 1847-1870; b) Y.-J. Yuan, Z.-T. Yu, D.-Q. Chen, Z.-G. Zou, *Chem. Soc. Rev.* **2017**, *46*, 603-631; c) W. T. Eckenhoff, R. Eisenberg, *Dalton Trans.* **2012**, *41*, 13004-13021.

[5] a) N. Armaroli, *Chem. Soc. Rev.* **2001**, *30*, 113-124; b) A. Barbieri, G. Accorsi, N. Armaroli, *Chem. Commun.* **2008**, 2185-2193; c) S. Otto, M. Grabolle, C. Förster, C. Kreitner, U. Resch-Genger, K. Heinze, *Angew. Chem. Int. Ed.* **2015**, *127*, 11735-11739; d) M. S. Lazorski, F. N. Castellano, *Polyhedron* **2014**, *82*, 57-70.

[6] a) M. Heberle, S. Tschierlei, N. Rockstroh, M. Ringenberg, W. Frey, H. Junge, M. Beller, S. Lochbrunner, M. Karnahl, *Chem. Eur. J.* **2017**, *23*, 312-319; b) E. Mejía, S.-P. Luo, M. Karnahl, A. Friedrich, S. Tschierlei, A.-E. Surkus, H. Junge, S. Gladiali, S. Lochbrunner, M. Beller, *Chem. Eur. J.* **2013**, *19*, 15972-15978; c) S. Tschierlei, M. Karnahl, N. Rockstroh, H. Junge, M. Beller, S. Lochbrunner, *ChemPhysChem* **2014**, *15*, 3709-3713; d) S.-P. Luo, E. Mejía, A. Friedrich, A. Pazidis, H. Junge, A.-E. Surkus, R. Jackstell, S. Denurra, S. Gladiali, S. Lochbrunner, M. Beller, *Angew. Chem. Int. Ed.* **2013**, *52*, 419-423; e) Y. Zhang, M. Heberle, M. Wachtler, M. Karnahl, B. Dietzek, *RSC Adv.* **2016**, *6*, 105801-105805; f) S. Fischer, D. Hollmann, S. Tschierlei, M. Karnahl, N. Rockstroh, E. Barsch, P. Schwarzbach, S.-P. Luo, H. Junge, M. Beller, S. Lochbrunner, R. Ludwig, A. Brückner, *ACS Catal.* **2014**, *4*, 1845-1849.

[7] a) Y. Zhang, M. Schulz, M. Wächtler, M. Karnahl, B. Dietzek, *Coord, Chem. Rev.* **2018**, *356*, 127-146; b) K. Saito, T. Arai, N. Takahashi, T. Tsukuda, T. Tsubomura, *Dalton Trans.* **2006**, 4444-4448; c) J. Windisch, M. Orazietti, P. Hamm, R. Alberto, B. Probst, *ChemSusChem* **2016**, *9*, 1719-1726; d) J. Kim, D. R. Whang, S. Y. Park, *ChemSusChem* **2017**, *10*, 1883-1886; e) M. Sandroni, M. Kayanuma, M. Rebarz, H. Akdas-Kilig, Y. Pellegrin, E. Blart, H. Le Bozec, C. Daniel, F. Odobel, *Dalton Trans.* **2013**, *42*, 14628-14638; f) S.-M. Kuang, D. G. Cuttell, D. R. McMillin, P. E. Fanwick, R. A. Walton, *Inorg. Chem.* **2002**, *41*, 3313-3322; g) A. Kaeser, M. Mohankumar, J. Mohanraj, F. Monti, M. Holler, J.-J. Cid, O. Moudam, I. Nierengarten, L. Karmazin-Brelot, C. Duhayon, B. Delavaux-Nicot, N. Armaroli, J.-F. Nierengarten, *Inorg. Chem.* **2013**, *52*, 12140-12151; h) M. Nishikawa, D. Kakizoe, Y. Saito, T. Ohishi, T. Tsubomura, *Bull. Chem. Soc. Jpn.* **2017**, *90*, 286-288; i) C. L. Linfoot, M. J. Leitl, P. Richardson, A. F. Rausch, O. Chepelin, F. J. White, H. Yersin, N. Robertson, *Inorg. Chem.* **2014**, *53*, 10854-10861; j) K. Soulis, C. Gourlaouen, C. Daniel, A. Quatela, F. Odobel, E. Blart, Y. Pellegrin, *Polyhedron* **2018**, *140*, 42-50; k) A. J. J. Lennox, S. Fischer, M. Jurrat, S.-P. Luo, N. Rockstroh, H. Junge, R. Ludwig, M. Beller, *Chem. Eur. J.* **2016**, *22*, 1233-1238; l) M. D. Weber, M. Viciano-Chumillas, D. Armentano, J. Cano, R. D. Costa, *Dalton Trans.* **2017**, *46*, 6312-6323.

[8] a) M. W. Blaskie, D. R. McMillin, *Inorg. Chem.* **1980**, *19*, 3519-3522; bD. R. McMillin, M. T. Buckner, B. T. Ahn, *Inorg. Chem.* **1977**, *16*, 943-945; cD. R. McMillin, J. R. Kirchhoff, K. V. Goodwin, *Coord. Chem. Rev.* **1985**, *64*, 83-92; d) F. N. Castellano, M. Ruthkosky, G. J. Meyer, *Inorg. Chem.* **1995**, *34*, 3-4; e) L. X. Chen, G. Jennings, T. Liu, D. J. Gosztola, J. P. Hessler, D. V. Scaltrito, G. J. Meyer, *J. Am. Chem. Soc.* **2002**, *124*, 10861-10867; f) G. B. Shaw, C. D. Grant, H. Shirota, E. W. Castner, G. J. Meyer, L. X. Chen, *J. Am. Chem. Soc.* **2007**, *129*, 2147-2160; g) N. A. Gothard, M. W. Mara, J. Huang, J. M. Szarko, B. Rolczynski, J. V. Lockard, L. X. Chen, *J. Phys. Chem. A.* **2012**, *116*, 1984-1992.

[9] a) M. W. Mara, K. A. Fransted, L. X. Chen, *Coord. Chem. Rev.* **2015**, *282–283*, 2-18; b) M. Iwamura, S. Takeuchi, T. Tahara, *Acc. Chem. Res.* **2015**, *48*, 782-791; c) M. Iwamura, H. Watanabe, K. Ishii, S. Takeuchi, T. Tahara, *J. Am. Chem. Soc.* **2011**, *133*, 7728-7736.

[10] a) A. K. Ichinaga, J. R. Kirchhoff, D. R. McMillin, C. O. Dietrich-Buchecker, P. A. Marnot, J. P. Sauvage, *Inorg. Chem.* **1987**, *26*, 4290-4292; b) C. C. Phifer, D. R. McMillin, *Inorg. Chem.* **1986**, *25*, 1329-1333; c) M. K. Eggleston, D. R. McMillin, K. S. Koenig, A. J. Pallenberg, *Inorg. Chem.* **1997**, *36*, 172-176; d) C. E. McCusker, F. N. Castellano, *Inorg. Chem.* **2013**, *52*, 8114-8120; e) O. Green, B. A. Gandhi, J. N. Burstyn, *Inorg. Chem.* **2009**, *48*, 5704-5714; f) M. T. Miller, P. K. Gantzel, T. B. Karpishin, *J. Am. Chem. Soc.* **1999**, *121*, 4292-4293.

[11] a) R. S. Khnayzer, C. E. McCusker, B. S. Olaiya, F. N. Castellano, *J Am Chem Soc* **2013**, *135*, 14068-14070; b) A. Edel, P. A. Marnot, J. P. Sauvage, *Nouv. J. Chim* **1984**, *8*, 495-499.

[12] a) M. Karnahl, *Bunsen-Magazine* **2015**, *17*, 232-238; b) C. K. Prier, D. A. Rankic, D. W. C. MacMillan, *Chem. Rev.* **2013**, *113*, 5322-5363; c) D. M. Schultz, T. P. Yoon, *Science* **2014**, *343*.

[13] T. Tsubomura, K. Kimura, M. Nishikawa, T. Tsukuda, *Dalton Trans*. **2015**, *44*, 7554-7562.

[14] K. Kubiček, S. Thekku Veedu, D. Storozhuk, R. Kia, S. Techert, *Polyhedron* **2017**, *124*, 166-176.

[15] M. Schulz, F. Droge, F. Herrmann-Westendorf, J. Schindler, H. Gorls, M. Presselt, *Dalton Trans.* **2016**, *45*, 4835-4842.

[16] a) J. Yano, V. K. Yachandra, *Photosynth. Res.* **2009**, *102*, 241-254; b) U. Bergmann, P. Glatzel, *Photosynth. Res.* **2009**, *102*, 255; c) J. K. Kowalska, F. A. Lima, C. J. Pollock, J. A. Rees, S. DeBeer, *Isr. J. Chem.* **2016**, *56*, 803-815; d) C. J. Pollock, K. Grubel, P. L. Holland, S. DeBeer, *J. Am. Chem. Soc.* **2013**, *135*, 11803-11808; e) J. A. Rees, V. Martin-Diaconescu, J. A. Kovacs, S. DeBeer, *Inorg. Chem.* **2015**, *54*, 6410-6422.

[17] a) C. Bressler, M. Chergui, *Annu. Rev. Phys. Chem* **2010**, *61*, 263-282; b) L. X. Chen, X. Zhang, *J. Phys. Chem. Lett.* **2013**, *4*, 4000-4013.

[18] F. A. Lima, C. J. Milne, D. C. V. Amarasinghe, M. H. Rittmann-Frank, R. M. v. d. Veen, M. Reinhard, V.-T. Pham, S. Karlsson, S. L. Johnson, D. Grolimund, C. Borca, T. Huthwelker, M. Janousch, F. v. Mourik, R. Abela, M. Chergui, *Rev. Sci. Instrum.* **2011**, *82*, 063111.

[19] G. Gavrila, P. Wernet, K. Godehusen, C. Weniger, E. T. J. Nibbering, T. Elsaesser, W. Eberhardt, P. Corkum, S. Silvestri, K. A. Nelson, E. Riedle, R. W. Schoenlein, *Ultrafast Phenomena XVI: Proceedings of the 16th International Conference*, Springer Berlin Heidelberg, **2009**, pp. 505-507.

[20] a) D. Göries, B. Dicke, P. Roedig, N. Stübe, J. Meyer, A. Galler, W. Gawelda, A. Britz, P. Geßler, H. S. Namin, A. Beckmann, M. Schlie, M. Warmer, M. Naumova, C. Bressler, M. Rübhausen, E. Weckert,

A. Meents, *Rev. Sci. Instrum.* **2016**, *87*, 053116; b) A. Britz, T. A. Assefa, A. Galler, W. Gawelda, M. Diez, P. Zalden, D. Khakhulin, B. Fernandes, P. Gessler, H. Sotoudi Namin, A. Beckmann, M. Harder, H. Yavas, C. Bressler, *J. Synchrotron. Radiat.* **2016**, *23*, 1409-1423.

[21] L. Stebel, M. Malvestuto, V. Capogrosso, P. Sigalotti, B. Ressel, F. Bondino, E. Magnano, G. Cautero, F. Parmigiani, *Rev. Sci. Instrum.* **2011**, *82*, 123109.

[22] a) M. Saes, F. v. Mourik, W. Gawelda, M. Kaiser, M. Chergui, C. Bressler, D. Grolimund, R. Abela, T. E. Glover, P. A. Heimann, R. W. Schoenlein, S. L. Johnson, A. M. Lindenberg, R. W. Falcone, *Rev. Scientific. Instrum.* **2004**, *75*, 24-30; b) G. Smolentsev, A. A. Guda, M. Janousch, C. Frieh, G. Jud, F. Zamponi, M. Chavarot-Kerlidou, V. Artero, J. A. van Bokhoven, M. Nachtegaal, *Faraday Discuss.* **2014**, *171*, 259-273; c) G. Smolentsev, A. Guda, X. Zhang, K. Haldrup, E. S. Andreiadis, M. Chavarot-Kerlidou, S. E. Canton, M. Nachtegaal, V. Artero, V. Sundstrom, *J. Phys. Chem. C.* **2013**, *117*, 17367-17375.

[23] L. X. Chen, X. Zhang, J. V. Lockard, A. B. Stickrath, K. Attenkofer, G. Jennings, D.-J. Liu, *Acta Crys. A* **2010**, *66*, 240-251.

[24] T. Sato, S. Nozawa, K. Ichiyanagi, A. Tomita, M. Chollet, H. Ichikawa, H. Fujii, S. I. Adachi, S. Y. Koshihara, *J. Synchrotron. Radiat.* **2008**, *16*, 110-115.

[25] a) D. Moonshiram, C. Gimbert-Suriñach, A. Guda, A. Picon, C. S. Lehmann, X. Zhang, G. Doumy, A. M. March, J. Benet-Buchholz, A. Soldatov, A. Llobet, S. H. Southworth, *J. Am. Chem. Soc.* **2016,** 138, 10586-10596 ; b) D. Moonshiram, A. Guda, L. Kohler, A. Picon, S. Guda, C. S. Lehmann, X. Zhang, S. H. Southworth, K. L. Mulfort, *J. Phys. Chem. C.* **2016**, *120*, 20049-20057; c) D. Moonshiram, A. Picon, A. Vazquez-Mayagoitia, X. Zhang, M.-F. Tu, P. Garrido-Barros, J.-P. Mahy, F. Avenier, A. Aukauloo, *Chem. Comm.* **2017**, *53*, 2725-2728; d) G. Smolentsev, V. Sundström, *Coord. Chem. Rev.* **2015**, *304-305*, 117-132; e) S. E. Canton, K. S. Kjær, G. Vankó, T. B. van Driel, S.-i. Adachi, A. Bordage, C. Bressler, P. Chabera, M. Christensen, A. O. Dohn, A. Galler, W. Gawelda, D. Gosztola, K. Haldrup, T. Harlang, Y. Liu, K. B. Møller, Z. Németh, S. Nozawa, M. Pápai, T. Sato, T. Sato, K. Suarez-Alcantara, T. Togashi, K. Tono, J. Uhlig, D. A. Vithanage, K. Wärnmark, M. Yabashi, J. Zhang, V. Sundström, M. M. Nielsen, *Nat. Comm.* **2015**, *6*, 6359; f) S. E. Canton, X. Zhang, J. Zhang, T. B. van Driel, K. S. Kjaer, K. Haldrup, P. Chabera, T. Harlang, K. Suarez-Alcantara, Y. Liu, J. Pérez, A. Bordage, M. Pápai, G. Vankó, G. Jennings, C. A. Kurtz, M. Rovezzi, P. Glatzel, G. Smolentsev, J. Uhlig, A. O. Dohn, M. Christensen, A. Galler, W. Gawelda, C. Bressler, H. T. Lemke, K. B. Møller, M. M. Nielsen, R. Lomoth, K. Wärnmark, V. Sundström, *J. Phys. Chem. Lett.* **2013**, *4*, 1972-1976; g) D. Hayes, L. Kohler, R. G. Hadt, X. Zhang, C. Liu, K. Mulfort, L. X. Chen, *Chem. Sci.* **2018**; h) J. Huang, K. L. Mulfort, P. Du, L. X. Chen, *J. Am. Chem. Soc.* **2012**, *134*, 16472-16475; i) M. W. Mara, D. N. Bowman, O. Buyukcakir, M. L. Shelby, K. Haldrup, J. Huang, M. R. Harpham, A. B. Stickrath, X. Zhang, J. F. Stoddart, A. Coskun, E. Jakubikova, L. X. Chen, *J. Am. Chem. Soc.* **2015**, *137*, 9670-9684; j) C. Lamberti, J. A. van Bokhoven, in *X-Ray Absorption and X-Ray Emission Spectroscopy*, John Wiley & Sons, Ltd, **2016**, pp. 351-383; k) M. Chergui, *Struct. Dyn.* **2016**, *3*, 031001.

[26] S. Paria, O. Reiser, *ChemCatChem* **2014**, *6*, 2477-2483.

[27] J. L. DuBois, P. Mukherjee, T. D. P. Stack, B. Hedman, E. I. Solomon, K. O. Hodgson, *J. Am. Chem. Soc.* **2000**, *122*, 5775-5787.

[28] a) T. J. Penfold, S. Karlsson, G. Capano, F. A. Lima, J. Rittmann, M. Reinhard, M. H. Rittmann-Frank, O. Braem, E. Baranoff, R. Abela, I. Tavernelli, U. Rothlisberger, C. J. Milne, M. Chergui, *J. Phys. Chem. A.* **2013**, *117*, 4591-4601; b) L. X. Chen, G. B. Shaw, I. Novozhilova, T. Liu, G. Jennings, K. Attenkofer, G. J. Meyer, P. Coppens, *J. Am. Chem. Soc.* **2003**, *125*, 7022-7034.

[29] L. S. Kau, D. J. Spira-Solomon, J. E. Penner-Hahn, K. O. Hodgson, E. I. Solomon, *J. Am. Chem. Soc.* **1987**, *109*, 6433-6442.

[30] N. C. Tomson, K. D. Williams, X. Dai, S. Sproules, S. DeBeer, T. H. Warren, K. Wieghardt, *Chem. Sci.* **2015**, *6*, 2474-2487.

[31] a) T. E. Westre, P. Kennepohl, J. G. DeWitt, B. Hedman, K. O. Hodgson, E. I. Solomon, *J. Am. Chem. Soc.* **1997**, *119*, 6297-6314; b) J. A. Rees, R. Bjornsson, J. K. Kowalska, F. A. Lima, J. Schlesier, D. Sippel, T. Weyhermuller, O. Einsle, J. A. Kovacs, S. DeBeer, *Dalton Trans.* **2017**, *46*, 2445-2455; c) M. Roemelt, M. A. Beckwith, C. Duboc, M.-N. Collomb, F. Neese, S. DeBeer, *Inorg. Chem.* **2012**, *51*, 680-687; d) D. F. Leto, T. A. Jackson, *Inorg. Chem.* **2014**, *53*, 6179-6194.

[32] R. Giereth, W. Frey, H. Junge, S. Tschierlei, M. Karnahl, *Chem. Eur. J.* **2017**, *23*, 17432-17437.

[33] B. Ravel, M. Newville, *J. Synchrotron. Radiat.* **2005**, *12*, 537-541.

[34] J. J. Rehr, R. C. Albers, *Rev. Mod. Phys.* **2000**, *72*, 621-654.

[35] D. C. Koningsberger, R. Prins, *X Ray Absorption: Principles, Applications, Techniques of EXAFS, SEXAFS and XANES*, John Wiley & Sons, **1988**.

[36] F. Neese, *Wiley Interdiscip. Rev. Comput. Mol. Sci.* **2012**, *2*, 73-78.

[37] a) A. D. Becke, *J. Chem. Phys.* **1993**, *98*, 5648-5652; b) P. J. Stephens, F. J. Devlin, C. F. Chabalowski, M. J. Frisch, *J. Phys. Phys. Chem.* **1994**, *98*, 11623-11627.

[38] P. Coppens, I. V. Novozhilova, *Int. J. Quantum. Chem.* **2005**, *101*, 611-623.

[39] F. Weigend, R. Ahlrichs, *Phys. Chem. Chem. Phys.* **2005**, *7*, 3297-3305.

[40] aS. Grimme, J. Antony, S. Ehrlich, H. Krieg, *J. Chem. Phys.* **2010**, *132*, 154104; b) S. Grimme, S. Ehrlich, L. Goerigk, *J. Comput. Chem.* **2011**, *32*, 1456-1465.

[41] a) A. D. Becke, *Phys. Rev. A* **1988**, *38*, 3098-3100; b) J. P. Perdew, *Phys. Rev. B* **1986**, *33*, 8822-8824.

[42] C. Lee, W. Yang, R. G. Parr, *Phys. Rev. B* **1988**, *37*, 785-789.

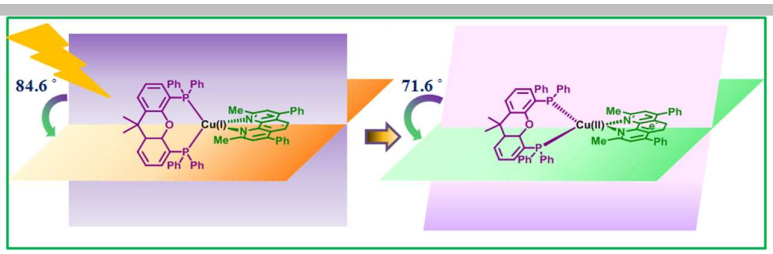

Light-induced electronic and geometric changes ~~within~~ of a heteroleptic Cu(I) photosensitizer are reported within the pico-microsecond time regime through time-resolved X-ray absorption spectroscopy.

D. Moonshiram*, P. Garrido-Barros, C. Gimbert-Suriñach, A. Picón, C. Liu, X. Zhang, M. Karnahl*, and A. Llobet*.

Page No. – Page No.

Elucidating the Nature of the Excited State of a Heteroleptic Copper Photosensitizer Using Time-Resolved X-ray Absorption Spectroscopy